Hydride abstraction by NO + from ethanol: Effects of collision energy and ion rotational state

Richard J. Green, Jun Qian, Ho-Tae Kim, and Scott L. Anderson

Citation: The Journal of Chemical Physics **113**, 3002 (2000); doi: 10.1063/1.1286917
View online: http://dx.doi.org/10.1063/1.1286917
View Table of Contents: http://scitation.aip.org/content/aip/journal/jcp/113/8?ver=pdfcov
Published by the AIP Publishing

Hydride abstraction by NO^+ from ethanol: Effects of collision energy and ion rotational state

Richard J. Green, Jun Qian, Ho-Tae Kim, and Scott L. Anderson[a)]
Chemistry Department, University of Utah, Salt Lake City, Utah 84112

(Received 5 April 2000; accepted 22 May 2000)

The effects of NO^+ rotational state and collision energy on the reaction $NO^+ + C_2H_5OH \rightarrow HNO + C_2H_4OH^+$ were studied in a guided-ion-beam instrument over the collision energy range from 50 meV to 3.7 eV. Integral cross sections for the reaction are presented. NO^+ is prepared in specific rotational levels ($N^+ = 0,1$ and $N^+ = 10$) by means of mass-analyzed threshold ionization. *Ab initio* calculations were used to probe stationary points on the potential energy surface. The reaction is sharply inhibited by collision energy, suggesting a bottleneck for reaction. If rotational energy had a similar effect, ~50% inhibition from $N^+ = 10$ excitation would be observed at low collision energy. Instead, rotation is found to have no effect within experimental error. A precursor complex mechanism is proposed to explain the results. © *2000 American Institute of Physics.* [S0021-9606(00)00232-4]

I. INTRODUCTION

Hydride (H^-) abstraction by NO^+ from hydrocarbons is a common reaction used in chemical ionization mass spectrometry. As a consequence, the thermal rate constants for many NO^+ + hydrocarbon reaction have been measured.[1] The rate constants are quite sensitive to hydrocarbon structure, with different isomers often showing two orders of magnitude difference. This report focuses on the collision and rotational energy effects on reaction of NO^+ with ethanol, studied over the energy range from near thermal to several electron volts.

The effects of ion rotational state on ion–molecule reactions have been studied for only a few reactions. The first such study was reported in 1968 by Chupka, Russell, and Refaey.[2] They used single-photon vacuum ultraviolet (VUV) photoionization to prepare H_2^+ with rotational quantum number (J^+) varying from 0 to 2. In the reaction: $H_2^+ + H_2 \rightarrow H_3^+ + H$, they found the effect of rotation to be less than 10%. Again, using VUV photoionization, Liao, Liao, and Ng[3] studied symmetric charge transfer between H_2^+ and H_2, using the autoionization propensity rules to control the ion rotational state over the range from $J^+ = 0$ to 2. Within their experimental uncertainty, no effects of rotational state were observed. In both experiments the rotational energy and angular momentum were small compared to the collision energy and collisional angular momentum. The rotational autoionization method is practically limited to preparation of H_2^+, where autoionization transitions are easily resolved and intense compared to the continuum.

Resonance-enhanced multiphoton ionization (REMPI) has been used for several rotationally state-selected ion–molecule reaction studies. Here, a single rotational state is used as the intermediate in a REMPI scheme, and rotational selection in the ion relies on propensity rules for rotational transitions in the ionization step. Because the photoelectron can carry away orbital angular momentum, the typical result is a narrow distribution of ion rotational states. For example, Fujii, Ebata, and Ito[4] used laser-induced fluorescence to study the nascent distribution of CO^+ produced using (2+1) REMPI via the $E\,^1\Pi$ intermediate state of CO. They found that ionization through the $N_i = 2$ intermediate state produced only ions in the $N^+ = 2$ level but that ionization via $N_i = 4$ produced ions in a mixture predominantly composed of $N^+ = 3,5$, and 7. Selection rules for MPI of diatomic molecules were derived by Xie and Zare.[5] Despite the fact that REMPI only rarely produces ions in a single rotational state, the technique is a useful, and relatively simple method to study the effects of the ion's rotation on reaction.

The clearest effects of rotational state have been observed by Gerlich and co-workers, capitalizing on their capability for studying reactions at subthermal collision energies—a regime in which rotational energy is a significant fraction of the available energy. Gerlich and Rox[6] used REMPI to produce CO^+ ($v = 0$, $N^+ = 0-7$) and studied the effects of both collision energy and rotational state on the association reaction: $CO^+(N^+) + 2CO \rightarrow (CO)_2^+ + CO$. The collision energy ranged down to about 0.5 meV, whereas the rotational energy could be varied from 0 to 10 meV. Both rotational and collision energy were found to decrease the association rate, and the effect was nonspecific, i.e., the decrease depends only on total energy. Gerlich, Jerke, and Schweizer[7] compared the effects of rotational excitation ($N^+ = 0-5$, $E_{rot} = 0-\sim 120$ meV) with vibrational excitation at a collision energy of 10 meV, on the reaction $H_2^+(v, N^+) + H_2 \rightarrow H_3^+ + H$. Both vibration and rotation were found to suppress reactivity, but rotation had roughly twice the effect for a given amount of energy. Glenewinkel-Meyer and Gerlich[8] recently reported another study of the $H_2^+ + H_2 \rightarrow H_3^+ + H$ reaction, in which both REMPI and pulsed-field ionization were used to prepare H_2^- ($v = 0-1$, $N^+ = 0-4$). They reported that rotational energy hinders reaction, and

a)Electronic mail: anderson@chemistry.utah.edu

that the effect is less than 10% for rotational excitation up to $N^+=5$. Using a potential surface calculated by Eaker and Schatz[9] they suggested that the hindrance was caused by one of four possible mechanisms: increased centrifugal barrier in the entrance channel, a rotational effect on the decay of the collision complex back to reactants, steric hindrance, or a transition to a nonreactive surface.

Mass-analyzed threshold ionization (MATI) is a variant on pulsed-field ionization, developed by Zhu and Johnson[10] and used by many groups for ion spectroscopy studies.[11–16] MATI allows formation of mass- and state-selected ions, with rotational selection possible in many cases. MATI spectra of the NO molecule have been reported by several groups including Mackenzie *et al.*,[17] using the $B\,^2\Pi$ intermediate state, and Sato and Kimura[18] using the $A\,^2\Sigma$ intermediate state. The first use of MATI for an ion–molecule reaction study was reported by Mackenzie *et al*. They studied the reaction H_2^+ $(N^+=0-3)+H_2\rightarrow H_3^++H$,[11,19,20] placing an upper limit on any rotational effect to be less than 10% at collision energies between 10 and 250 meV. This observation is consistent with the experiments by Chupka, Russell, and Refaey,[2] and by Gerlich and co-workers.

To date, the range of systems for which ion rotational effects have been studied is narrow, comprising only symmetric diatomic association and proton transfer reactions. The $NO^++C_2H_5OH$ system reported on here differs in some significant ways. For symmetric systems, the degeneracy of the M^++M and $M+M^+$ reactant charge states guarantees that nonadiabatic behavior will be possible as the intermolecular interaction mixes the asymptotic states. The ionization energy of NO is more than 1 eV lower than that of ethanol, thus it is less likely that nonadiabatic effects are important. The neutral reactant has many more degrees of freedom, allowing reactions mediated by longer-lived collision complexes. In addition, because the neutral reactant is a physically larger molecule, the moments of inertia in any complexes that form are substantially larger than those in diatomic–diatomic systems. This changes the relation between angular momentum and rotational energy as complexes form and rearrange. Finally, both neutral and ion in our system have significant dipole moments, raising the possibility of stronger anisotropic effects.

In addition to the previous studies of ion rotational state effects, several groups have studied the effects of the rotational energy of the neutral reactant in ion–molecule reactions. In general, these studies have either used *para* and normal H_2 as the neutral, or have varied the temperature of the neutral reactant. In the first category, Marquette, Rebrion, and Rowe studied the reaction of N^+ with H_2[21] concluding that neutral rotation is important in driving this endoergic reaction. The Gerlich group has studied a number of M^++H_2 reactions using this approach.[22] Their study of N^++H_2 compared the effects of rotation and collision energy. The results are consistent with those of Marquette, Rebrion, and Rowe and show that rotation is at least as effective as collision energy in overcoming the activation barrier. In reaction of CH_3^+ and CD_3^+ with hydrogen and helium, Gerlich and Kaeffer have studied the effect of neutral rotation upon the ternary rate coefficient.[23] They found that rotation inhibits reaction; however, it does so by a factor of four times less than predicted by theory.

Viggiano and co-workers have reported several studies in their selected-ion flow drift tube (SIFDT) in which the effects of the neutral reactant's rotation were studied by independently varying the temperature and the average kinetic energy (i.e., drift velocity) of the reactants.[24,25] For example, in the reaction of O^+ with HD,[25] it was found that the overall rate constant was independent of temperature or average kinetic energy in the range studied, but that the branching ratio into OD^+ and OH^+ at a given average kinetic energy varied as a function of temperature. This effect was attributed to the changes in HD rotational temperature. The theoretical work of Dateo and Clary on the effects of rotation on long-range capture[26] accounted for the observations. The physical picture is that the HD has different centers of mass and polarizability, causing the H end to be oriented toward the O^+. Rotation decreases the orientation effect. Another example was found in a study of $Kr^+(^2P_{3/2})$ with HD, in which it was found that the KrH^-/KrD^+ branching ratio was affected by rotation in the opposite sense from the effect of kinetic energy.[27] Viggiano and co-workers have recently reviewed studies of a variety of reactions using this method.[28]

The reaction studied here is hydride abstraction by NO^+ from ethanol:

$$NO^+(N^+)+C_2H_5OH\rightarrow HNO+C_2H_5O^+. \tag{1}$$

The collision energy was varied from 50 meV to 3.7 eV, and the reactivity of two NO^+ rotational states was examined. The first state is an unresolved mixture of $N^+=0$ and 1, and the second state is $N^+=10$. The rotational and centrifugal distortion constants of NO^+ are 1.997 cm^{-1} and 5.64 $\times10^{-6}$ cm^{-1}, respectively,[29] thus the energies of the reactant states are 0, 3.98, and 218.6 cm^{-1}, or 0, ~0.5, and ~27 meV. At our lowest collision energy, the $N^+=10$ rotational energy is about 50% of the collision energy. The thermal energy in the EtOH reactant is 76 meV, approximately equally divided between rotation and vibration. In terms of total energy, exciting $N^+=10$ increases the total energy at our lowest experimental point by 21%.

Williamson and Beauchamp[30] have studied reaction (1) in an ion-cyclotron-resonance spectrometer (ICR), and Spanel and Smith[31] studied the reaction in a (SIFDT). The results of these studies are discussed in the following.

II. EXPERIMENTAL METHODOLOGY

The guided-ion-beam instrument used in these studies has been described previously, along with calibration and data analysis procedures.[32–35] For this study, reactant NO^+ is prepared using a $1+1'$ photon MATI scheme. The first photon excites the neutral molecule to the $A\,^2\Sigma$ state of NO via a particular rotational transition in the 0–0 band. The second photon pumps the *A*-state molecules into an ensemble of high-lying Rydberg states that converge upon the ion rotational state of interest. The Rydberg molecules are then field ionized to generate NO^+ in the desired rotational state. To produce low rotational state ions, we excite the $R_{21}(0.5)$ transition to the *A* state, and to produce high N^+ we excite the $R_{21}(8.5)$ line. Figure 1 shows MATI spectra from both

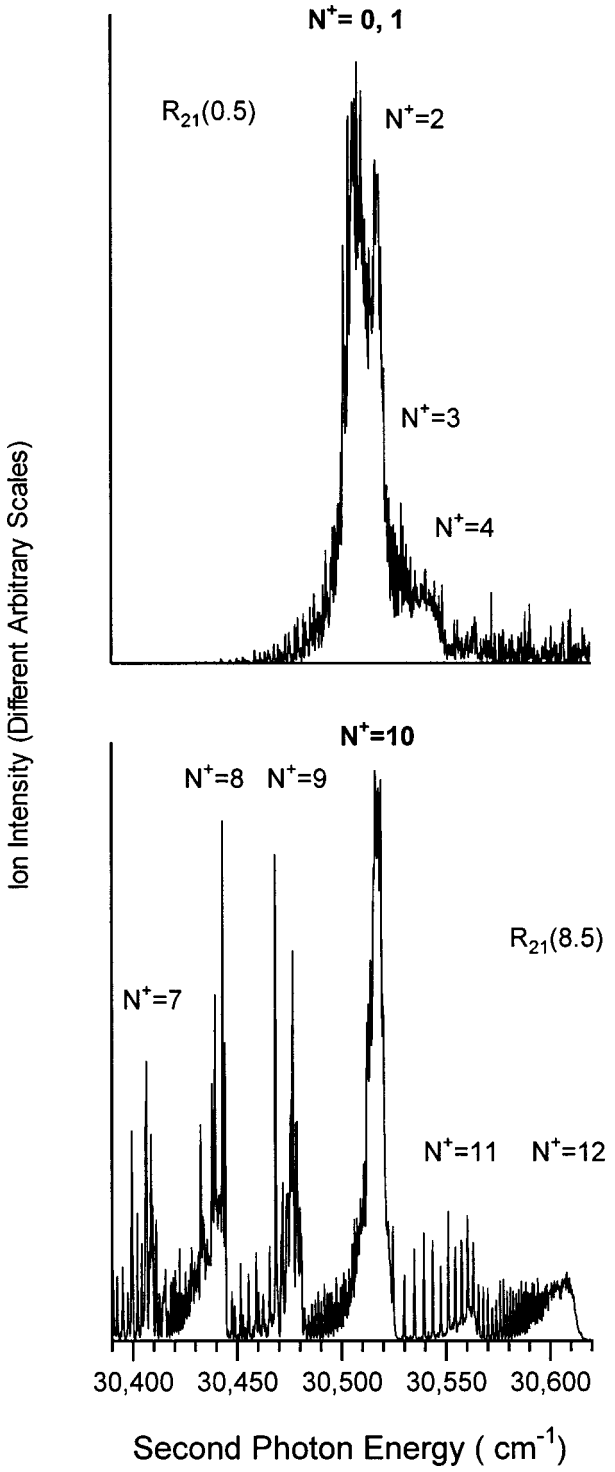

FIG. 1. MATI spectra of NO via the $A\,^2\Sigma$ intermediate state. The sharp structure is the *np* Rydberg series converging on the ionization threshold for each rotational state of the ion. Ions are produced by scanning the second laser while the first laser excites a rotational line of the 0–0 band of the $A\,^2\Sigma - X\,^2\Pi$ transition. In the upper spectrum the first laser excites the $R_{21}(0.5)$ line. In the lower, it excites $R_{21}(8.5)$.

intermediate states. The sharp structure is the *np* series of high-lying Rydberg states converging to each ion rotational state. In the following we report reactivity of NO^+ in the unresolved mixture of $N^+=0$ and 1, and in $N^+=10$.

The Rydberg excitation process also generates ions that are not in the desired state, and these are rejected by a weak electric field prior to field ionization. Neutral NO is injected into the source as a pulsed, seeded beam. Multiphoton excitation is carried out between a pair of plates separated by 12.7 mm, with apertures to allow beam transmission, and with a series of intermediate electrodes that allow us to create a uniform field across the interplate gap. In the first 100 ns after the laser pulse, this region is field free, and then a field of approximately 1.5 V/cm is applied, oriented such that it retards the prompt ions produced in the laser pulse. As reported by Sato and Kimura[18] we find that the MATI signal is enhanced by the presence of this separation field and the field strength is adjusted to maximize signal. Vrakking and Lee[36] reported enhancement in the lifetime of high-lying Rydberg states in the presence of an electric field, which they attribute to *l* mixing induced by the field. Merkt and Zare have published a model for such a mechanism.[37]

The NO neutrals, including the high-lying Rydbergs, are not retarded, and pass into the second region of the source (7.6 mm long), where the Rydbergs are field ionized by a 20 ns, 50 V/cm pulse. The resulting MATI ions are focused by a set of lenses into a quadrupole ion guide, where a combination of focusing properties and time-of-flight (TOF) gating is used to velocity filter the beam and reject any prompt ions or ion fragments that might be present. The ions are next injected into a two-section octapole ion guide. In the first section, the collision energy is set and the NO^+ beam is guided through a 11.3 cm cell containing 0.1 mTorr of ethanol vapor (Quantum Chemical Company). To allow correction for reactions occurring outside the cell, measurements are also made with the same ethanol flow rate dumped directly into the vacuum chamber surrounding the cell. Product ions, along with unreacted NO^+, are collected by the octapole and passed into the second section of the ion guide. For these experiments this section was operated at a dc potential $\sim$1.5 V below that of the first section of the guide to improve collection of slow product ions. TOF through the guide system is used to measure the primary ion beam velocity distribution, and also to measure recoil velocity distributions for the product ions. Finally, the ions are collected and injected into a conventional quadrupole mass filter, and counted by a Daly detector/multichannel scalar combination. The cross sections are calculated from the product signal with ethanol filling the cell minus the signal with the ethanol flow diverted into the chamber. This subtraction compensates for any reactions taking place in the second octapole segment.

The chief problem with using MATI for rotational state selection is that angular momentum conservation dictates that to produce rotationally hot NO^+, the NO neutral precursor must also be rotationally hot. MATI also requires that the neutrals have a well-defined and reasonably high velocity to allow Rydberg/ion separation, dictating use of a seeded neutral beam. The concomitant rotational cooling makes production of high-N^+ state ions quite difficult. In the experiments here, we are able to produce substantial intensities ($\sim$5000 ions/s) for the $N^+=0,1$ beam, but only 200–300 ions/s for $N^+=10$. In order to eliminate any intensity-dependent systematic errors in comparing the $N^+=0,1$ and $N^+=10$ results, the laser was attentuated for the $N^+=0,1$ experiments

so that the ion beam intensity was equally poor for the entire data set.

Two products are observed in the reaction, at m/q 45 and m/q 47. The former is the major $C_2H_5O^+$ product, and, as in the ICR experiments of Williamson and Beauchamp,[30] the latter is attributed to a secondary reaction of the major product ion: $C_2H_5O^+ + C_2H_5OH \rightarrow C_2H_7O^+ + C_2H_4O$ ($\Delta H_{rxn} = -0.04$ eV). It is not practical to eliminate the secondary reaction, because the primary reaction generates some $C_2H_5O^+$ that is very slow in the laboratory frame, with high secondary reaction probability. Owing to the very low primary ion intensity, we did not attempt to measure the pressure dependence of the cross sections. Taking advantage of the fact that the only source of m/q 47 is secondary reaction of the primary product ion, we simply summed the m/q 47 and 45 signals to calculate the reaction cross section.

One potentially important issue is the possibility that rotationally inelastic collisions might perturb the reactant rotational state distributions prior to reaction. We can estimate the importance of nonreactive collisions by observing changes in the NO^+ beam pulse when the scattering cell is filled with ethanol vapor. Reactive collisions lead to loss of NO^+ intensity, but nonreactive collisions lead to NO^+ that is shifted to lower laboratory energies relative to the sharp reactant beam pulse. We estimate that the total fraction of ions having a single collision ranges from 34% at low energies to 24% at high energies. This fraction includes reactive collisions and any elastic or inelastic collisions that result in significant change in the lab velocity. Based on these fractions, we estimate that ~10% of the reactive signal could result from reactant ions that had previously undergone a nonreactive collision. While 10% multiple collisions is undesirable, it would not obscure a substantial rotational effect on the reaction cross section. Ordinarily we operate at lower scattering gas densities to avoid the issue, but the low primary beam intensity and small reaction cross section mandate high target densities.

Figure 2 shows a velocity profile of the reactant MATI beam at 0.3 eV nominal collision energy and also a Gaussian fit used to calculate the mean collision energy ($\langle E_{\mathrm{col}} \rangle = 0.304$ eV). The beam velocity distribution is determined by a number of factors, including the potential distributions in the ionization volume and scattering octapole, the homogeneity of the field ionization pulse, and the neutral precursor velocity distribution. Because factors such as the laser alignment, pulsed valve-laser timing, surface potentials, and time/spatial profile of the field ionization pulse can vary from experiment to experiment, the actual collision energy distribution associated with a particular nominal energy varies. The variations can be large (0.2 eV) if the laser is realigned or some experimental setting is changed, but during the course of one set of experiments the collision energy is generally quite stable (20–30 meV). Multiphoton ionization produces beams with both shot-to-shot and long-term intensity fluctuations. To compensate for shot-to-shot fluctuations, lengthy signal averaging is required, and to avoid systematic errors from the long term drift, the averaging is done as a set of quick cycles through a complete data set (primary and product ion intensities and TOFs as a function of collision energy for scattering cell empty and full). Ordinarily, we simply average data from each cycle together, and because the cycle-to-cycle collision energy distribution is reasonably constant (20–30 meV), the effect on collision energy resolution is small.

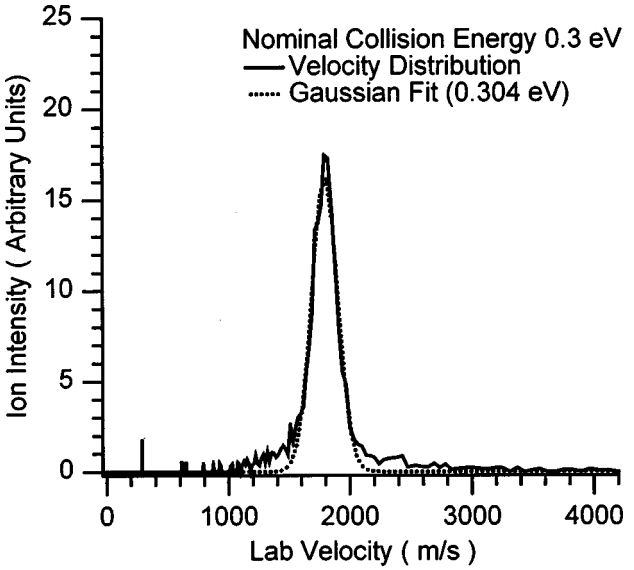

FIG. 2. The velocity distribution of the reactant NO^+ ($N^+ = 0,1$) MATI beam at a nominal energy of 0.3 eV, together with a Gaussian fit.

For the $NO^+ + EtOH$ reaction at low collision energies, the cross section is such a steep function of the collision energy that even small shifts in the collision energy distribution can lead to significant errors in comparing data at the same nominal energy. We were, therefore, forced to abandon averaging, and treat each acquisition cycle separately. For each cycle we have analyzed the primary beam TOF, rejecting any cycles where the reactant velocity distribution was broadened or distorted. The cross section for each cycle is then determined from the primary and product signals from that cycle, and plotted against the collision energy taken as the mean of a Gaussian fit to the NO^+ velocity distribution measured during that cycle. This procedure results in having a well-defined collision energy associated with each cross-section point, but with minimal signal averaging to compensate for shot-to-shot intensity fluctuations. The combination of low primary intensities and short averaging times results in badly scattered cross-section points (including negative apparent cross sections due to the subtraction procedure, described previously). Conclusions regarding the collision energy and rotational state dependence of the cross sections must, therefore, be taken from fits to the data.

III. RESULTS

Cross sections for hydride abstraction are shown in Fig. 3 over the collision energy range from ~50 to ~500 meV. The inset shows the full range of collision energy studied (~50 meV to ~3.7 eV). Data are shown for reaction of a mixture of $N^+ = 0$ and 1 (low N^+), and for $N^+ = 10$ (high N^+). At low collision energy, the cross section approaches 25 $Å^2$, but falls off rapidly as the collision energy increases.

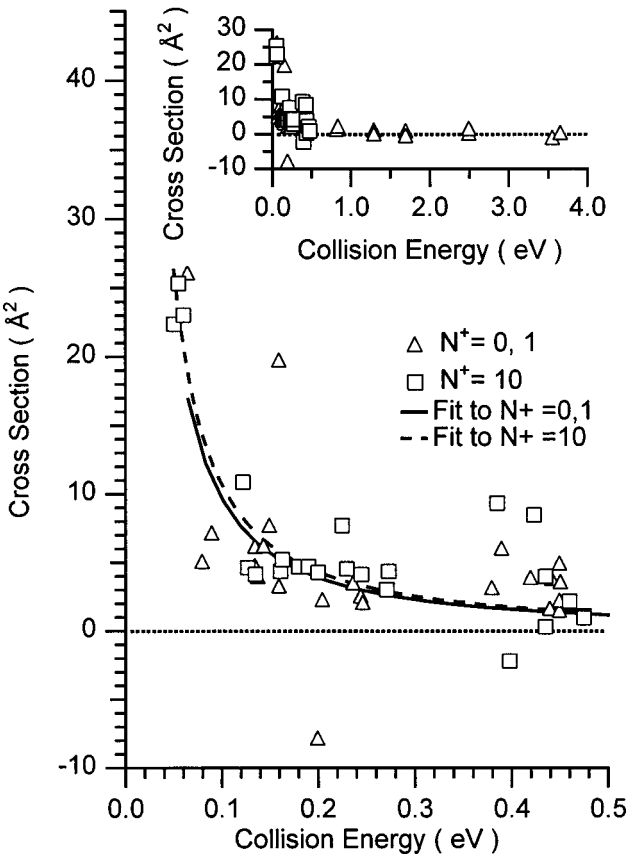

FIG. 3. A scatter plot of the cross section for the hydride abstraction reaction as a function of collision energy for the rotational states studied. The inset shows the full collision energy range studied, while the main figure shows the low energy range. The curves are power laws fits to the data ($\sigma = K \cdot E_{\mathrm{col}}^{-1.3}$). See the text for details.

By $E_{\mathrm{col}} = 1.5$ eV the cross section is essentially zero within the rather poor sensitivity limits dictated by the low $N^+ = 10$ intensity.

The thermal rate constant reported by Williamson and Beauchamp[30] (8.0×10^{-10} cm^3/molecules s) is 30% of the capture rate constant for ion–ethanol collisions, calculated using Troe's statistical adiabatic channel theory.[38] The result of Spanel and Smith[31] (5×10^{-10} cm^3/molecules s) corresponds to 20% of the capture rate. Our cross section at the lowest experimental energy (~50 meV) is only 7% of the capture cross section. By extrapolating the functional fit (see the following) of the collisional energy dependence of our cross section to thermal energies and averaging over a Maxwell–Boltzmann distribution of collision energies, we derive a rate constant of 4.3×10^{-10} cm^3/molecules s, in reasonable agreement with the result of Spanel and Smith. The origin of the discrepancy with the rate of Williamson and Beauchamp is not clear, but vibrational excitation seems a likely culprit. In our experiment and in the SIFDT experiments of Spanel and Smith, the reactant ions are in their vibrational ground state, while in the ICR experiments of Williamson and Beauchamp, the NO^+ may have had some vibrational excitation. Indeed, estimating the ionization Franck–Condon factors from the photoelectron spectrum[39] of NO, suggests that electron-impact ionization will produce substantial populations of $v^+ = 0-4$. Even modest vibrational enhancement would account for the higher rate constant measured in the ICR.

Comparison of the data shows immediately that there is no major effect of the rotational states studied. The scatter in the data points is so large, however, that a small effect would be obscured. Indeed, the confidence limits on an unconstrained statistical analysis (e.g., two dimensional Kolmogorov–Smirnov[40]) are still too large to be helpful in deciding if there might be a small rotational effect. To look for possible small effects, we adopted the following procedure. We start with the assumption that the cross sections for low and high N^+ are, in fact, identical. We then fit the combined set of low and high N^+ data points to a single power law expression: $\sigma = K \cdot E_{\mathrm{col}}^{n}$, with best fit parameters $K = 0.52 \pm 0.07$ and $n = -1.3$. This functional form was chosen because it gives an acceptable fit with only two parameters. Note that it is thermal averaging of this expression that gives a rate constant in good agreement with the Spanel and Smith SIFDT experiment, confirming that the cross section really does rise sharply at very low collision energies.

We then fit the low N^- and high N^+ distributions independently using the single parameter expression: $\sigma = K \cdot E_{\mathrm{col}}^{-1.3}$, where the exponent ($-1.3$) was taken from the fit to the combined data set. In essence, this analysis makes the assumption that rotation might affect the magnitude of the cross section, but not the collision energy dependence. The values of the scale factor K are 0.50 ± 0.14 for low N^+, and 0.54 ± 0.07 for high N^+, where the uncertainties are 95% confidence limits. The small difference in scale factors is equivalent to 0.60 Å^2 at 0.1 eV and is certainly not significant. Similar analysis was done in which we ignored outlying points in the fits. Because of the scatter in the data, we cannot rule out the possibility that rotational energy may enhance reactivity, i.e., ignoring the outliers causes the K value for high-N^+NO^+ at low energy to be ~20% larger than that for low N^+.

The conclusion is that rotation certainly does not inhibit reaction for the states studied, but we cannot rule out the possibility that rotation slightly enhances reactivity. In any case, any effect is certainly within the experimental error. We also cannot rule out the unlikely case of a nonmonotonic dependence on rotational state that accidentally vanishes at the states studied. The lack of rotational dependence is in contrast to the strong inhibitory effect of collision energy. At our lowest collision energy (50 meV), adding 27 meV of rotational energy ($N^+ = 10$) has no detectable effect. Adding the same amount of collision energy decreases the cross section by nearly a factor of 2. The collision energy effect is particularly striking in light of the fact that, on average, the thermal energy of the ethanol reactant is 76 meV. Thus, 27 meV represents only a 21% increase in the total energy.

One issue in developing a reaction mechanism is whether H^+ is abstracted from methyl, methylene, and/or hydroxyl positions on EtOH. The most energetically favorable $C_2H_5O^+$ product is CH_3CHOH^+, and in this case the reaction is exoergic by ~16 kcal/mol.[41] Williamson and Beauchamp[30] showed that for their thermal energy collisions, hydride abstraction occurred only from the alkyl moiety. Our

lowest energies are in the range present in ICR experiments, thus abstraction from the alkyl moiety should dominate for us, as well. To get a rough estimate of the relative difficulty of abstracting H^- from CH_3, OH, and CH_2 groups, we compared the energies of single point calculations at the MP2/6-31G* level using GAUSSIAN 98[42] for CH_3CHOH^+, $CH_3CH_2O^+$, and $CH_2CH_2OH^+$ where the structures were frozen in the ethanol geometry. In all cases, the singlet states are substantially lower in energy than the triplets. Among the singlets, CH_3CHOH^+ is more stable than $CH_2CH_2OH^+$ by 1.75 eV, and more stable than $CH_3CH_2O^+$ by 4.4 eV. These frozen geometry calculations certainly do not give the true difference in reaction path energetics for abstraction from the three sites, however, they do suggest that abstraction from the methylene site probably dominates the reaction mechanism, at least in the low collision energy range of greatest interest.

IV. DISCUSSION

At high collision energies, reaction mechanisms tend to be direct, because binding energies are too weak compared to the collision energy to stabilize long-lived complexes. The small cross section observed at high energies indicates that direct H^- abstraction has an efficiency less than 1% at energies over 1.5 eV. The balance of the discussion will focus on the reaction mechanism in the more interesting low-collision-energy regime.

From a dynamical point of view, the most interesting observation is the unusually strong collision energy dependence. At low collision energies, ion–molecule reactions with no activation barriers often occur with cross sections that are a substantial fraction of the collision cross section. At our lowest collision energy, the experimental reaction efficiency, defined here as the ratio of the measured cross section to the capture cross section,[38] is roughly 7%. Efficiency at $E_{\mathrm{col}}=0.2$ eV has dropped to ~3.5%, and above 1 eV the efficiency is less than 1%.

Such a sharp decrease in reaction efficiency with increasing energy is usually the result of a bottleneck (tight transition state) that inhibits reaction. Reaction clearly proceeds with no activation energy, as shown by the E_{col} dependence of the cross section, thus the rate-limiting transition state for hydride abstraction (TS_{HA}) must be below the energy of the reactants. There are at least two ways in which a tight geometric constraint can result in reaction efficiency that decreases with increasing energy. For example, it might be that NO^+ must approach EtOH in the correct orientation for reaction to occur. Collisions at low energies might be efficient because long-range forces orient the reactants as they approach, while at high energies there is insufficient time for the long-range torques to have a significant effect. In the NO^+–EtOH system, however, this ''approach geometry'' scenario is unlikely. The dominant long-range force is the ion–dipole force that tends to orient EtOH. The dipole moment of ethanol is such that ion–dipole interaction favors orienting the hydroxyl O atom toward the ion, whereas one would expect that the reactive geometry must have one of the labile methylene H atoms directed at NO^+.

A more likely scenario involves a precursor complex. In ion–molecule systems, there often are weakly bound reactantlike structures that can support an intermediate complex. Generally, there is no energetic barrier to formation of such reactantlike complexes and the transition state (TS_R) separating reactants from the complex is loose—near the orbiting limit. If a precursor complex forms, it can either dissociate back to reactants via the loose transition state (TS_R), or pass through the rate-limiting transition state (TS_{HA}) and on to products.

MP2/6-31G* calculations were carried out to look for complexes in the $[NO–EtOH]^+$ system. Figure 4 shows the six complexes found and their energies relative to reactants, including zero point energy corrections. Both top and side views are shown except in the case of Ex1, where the heavy atoms are roughly coplanar. The complexes can be characterized as reactantlike (Er1, En2, En3), productlike (Ex1), and insertion complexes (I1, I2). Of these complexes, the reactantlike are the lowest in energy, and are obvious candidates to serve as precursor complexes.

All three reactantlike complexes have the NO cation complexed to the hydroxyl O atom—the most negatively charged atom in EtOH. En1 and En2 both have the more positive N atom in NO^+ coordinated to the O atom in EtOH, and the NO orientation is roughly parallel to the direction of the dipole moment in free EtOH. In this context it should be noted that EtOH has two conformers, calculated to be nearly isoenergetic ($\Delta E<5$ meV at both the MP2/6-31G* and G3 levels of theory). The barrier to interconversion is 43 meV at MP2/6-31G*. One conformer has OH oriented coplanar with the CC bond, as in En1, and the other has OH oriented such that the CCOH dihedral angle is ~65°, roughly as in En2. In essence, the En1 and En2 complexes have NO^+ coordinated in geometries that maximize ion–dipole and dipole–dipole forces for the two conformers of EtOH. In En3 the CCOH dihedral angle is reduced to ~10°, and more important, NO^+ is bound with its oxygen atom closest to the hydroxyl O atom, resulting in somewhat lower binding energy.

The fact that these reactantlike complexes have geometries that appear to maximize the ion–dipole (and for En1 and En2, the dipole–dipole) attractions, suggests that long-range forces during approach should tend to orient the reactants to maximize complex formation, with the specific complex formed depending on approach geometry. Note that the binding energies of these complexes are more than five times the collision energy over the entire dynamically interesting energy range ($E_{\mathrm{col}}<0.25$ eV). With these properties, formation of the reactantlike complexes is expected to be quite efficient, as required for a precursor mechanism.

En3 has the NO^+ moiety correctly oriented for nitrogen attack on the methylene CH bond, whereas En1 and En2 require more extensive rearrangement to allow hydride abstraction. Mechanistically, it is important to know whether the more stable En1 and En2 complexes can easily convert to En3. Rather than searching for the transition states for interconversion, we did a series of calculations on structures midway between En2 and En3, varying the distance and angle of NO relative to EtOH. The lowest energy geometry was only ~0.22 eV above the energy of En3, or 0.55 eV above En2,

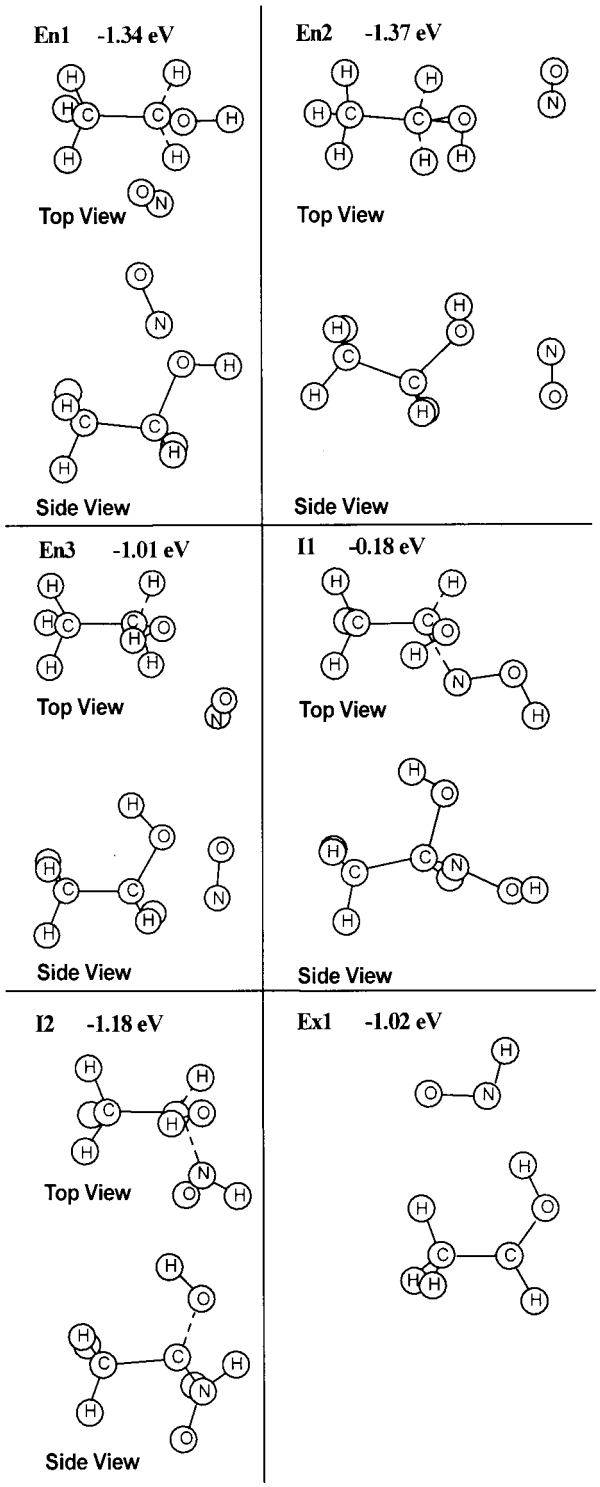

FIG. 4. Geometries of stable complexes optimized at the MP2/6-31G* level of theory. Reactantlike complexes (En1, En2, En3), insertion-type complexes (I1, I2), and a productlike complex (Ex1) are shown. A top and side view of each complex is shown with the exception of Ex1 in which the heavy atoms are roughly planar. The energy of each complex is shown relative to the energy of the separated reactants.

and its energy should be a reasonable upper limit on the energy of the true transition state. As this energy is well below the available energy in the complexes, it is clear that interconversion between complexes should be facile.

The other obvious question is whether the lifetimes for the reactantlike complexes are long enough to be mechanistically significant. To address this issue we performed Rice–Ramsperger–Kassel–Marcus (RRKM) calculations,[43] using scaled frequencies from the MP2/6-31G* calculations and assuming an orbiting transition state[44–46] for TS_R. At the lowest total energies in the experiment, both En1 and En2 complexes are quite long lived (tens of nanoseconds), and the lifetime is still hundreds of picoseconds at $E_{col}=0.25$ eV. En3, because it is less strongly bound and also less floppy, is shorter lived, with lifetimes ranging from a few nanoseconds at $E_{col}=0.05$ eV to a few picoseconds at 0.25 eV. These RRKM results neglect the rapid interconversion between complexes, and the true lifetime is determined by the aggregate density of states in the set of complexes. As most of the density is found in the En1 and En2 wells, the resulting lifetime should be at least hundreds of picoseconds over the energy range of interest ($E_{col}<0.25$ eV). The RRKM calculations also neglected the rate of the H^- abstraction reaction, however, the small experimental cross section suggests that this assumption is reasonable. Note that the fraction of the aggregate complex lifetime that is spent in each potential well depends on the ratios of the density of states in the wells. The fraction varies somewhat with energy and angular momentum, but is roughly 0.4, 0.6, and 0.003, for En1, En2, and En3, respectively.

The conclusion that the precursor complex lifetime is long is consistent with experiment. We have measured the axial recoil velocity distributions for the product ions, and while the small cross section and poor kinematics makes quantitative interpretation impossible, the measurements are consistent with forward–backward symmetric recoil velocities.[33] Such velocity distributions are a necessary condition for concluding that reaction is mediated by a complex with lifetime greater than a few picoseconds.

The above-mentioned considerations strongly suggest that formation of a long-lived precursor (i.e., the set of interconverting reactantlike complexes) is facile at low collision energies. Once the precursor has formed, the actual mechanism for hydride abstraction is unclear. For reaction at low energies, a likely mechanism is ''insertion–elimination,'' where NO^+ inserts in a methylene CH bond, followed by HNO elimination. Indeed, the very low reactivity observed at high collision energies, where direct reaction is expected to dominate, tends to suggest that direct abstraction is inefficient. In an insertion–elimination mechanism, the complexes I1 and I2 are likely candidates for insertion intermediates. Both complexes have NO inserted into a methylene CH bond; however, I2 is much lower in energy and can dissociate directly to $HNO+C_2H_5O^+$ products. I1, in contrast, is a high-energy geometry, and also would require HON→HNO isomerization to reach the ground state products. (The HON isomer is 2.17 eV higher in energy than HNO, thus we can exclude the $HON+C_2H_5O^-$ product channel.) Given these considerations, the rate-limiting transition state (TS_{HA}) for an insertion–elimination mechanism is almost certainly at the critical configuration for insertion to form I2.

The alternative to insertion–elimination is direct abstraction. As noted, direct abstraction is quite inefficient at high collision energies, but it is conceivable that there is a con-

certed abstraction pathway that might be efficient at low energies, where the collision time is long. In such a concerted mechanism, the transition state (TS_{HA}) would presumably be at the barrier for attack of NO^+ on the hydrogen, and the nascent HNO would not be chemically bonded to the CH_3CHOH^+ moiety. Products might either separate immediately, or possibly pass through a productlike complex such as Ex1. We did a number of calculations to probe the energetics of NO^+ attack on the methylene hydrogen. Optimizations were started with NO^+ positioned at several distances (ranging down to ~1.7 Å) and orientations relative to the methylene CH bond. These geometries all converged back to reactantlike complexes, suggesting that the transition state for this mechanism lies at short NO–EtOH separations (and high energy).

We made numerous attempts to optimize transition states for both insertion and direct abstraction. Optimizations were attempted using the transit-guided quasi-Newton and Berny algorithms, implemented in GAUSSIAN98. The only transition states found were for uninteresting motions such as torsions. The higher order saddle points found were substantially above the reactant energy, and therefore poor approximations to TS_{HA}, which must lie below the reactant energy. We also attempted to distort second-order saddle points into reasonable starting geometries for TS optimizations. All attempts failed.

For either mechanism, TS_{HA} must be a relatively compact structure with rotational constants not radically different from those of the precursor complexes. The real unknowns are the vibrational tightness of TS_{HA} and its energy with respect to reactants. The TS_{HA} transition state, particularly for an insertion reaction, is likely to be substantially stiffer than either En3 or I2. In contrast, the orbiting transition state (TS_R) is very loose, with rotations replacing the low frequency vibrations in the complexes. Because we have only estimates for the properties of TS_{HA}, we cannot calculate reaction efficiency using RRKM theory. Nonetheless, the qualitative picture suggests that vibrational stiffness should contribute to a substantial bottleneck inhibiting reaction.

It is also clear that some of the bottleneck must result from angular momentum conservation, as follows. As the precursor forms, the angular momentum of the collision must be converted to tumbling rotation of the complex, and because the moment of inertia in the complex is substantially lower than at the orbiting transition state (TS_R), considerable energy is tied up in rotation of the complex. In passage through a compact TS, such as TS_{HA}, this rotational energy is not available to drive reaction, whereas in dissociation back through TS_R, much of the rotational energy is converted back to translation to drive dissociation. As a consequence, reaction is suppressed in high angular momentum collisions. Because angular momentum increases with collision energy, reactivity tends to be inhibited by increasing energy.

We can estimate the maximum orbital angular momentum in collisions that can form complexes as $L_{max}=\mu\cdot v_{rel}\cdot b_{max}$, where μ is the reduced mass, v_{vel} is the relative velocity of the reactants, and b_{max} is the maximum impact parameter leading to capture. Given the assumption of the capture model, i.e., that all collisions with $L<L_{max}$ lead to capture, we can also estimate the average L. At our lowest collision energy (0.05 eV) L_{max} is ~200$\hbar$ and L_{avg} is ~140$\hbar$, but L_{avg} increases quite slowly with increasing E_{col}. Increasing the collision energy by a factor of 6 to 0.3 eV increases L_{max} and L_{avg} by only a factor of 1.5, but decreases the reaction cross section by an order of magnitude. For a collision at 0.05 eV with $L=L_{avg}$, the energy going into tumbling rotation of the complex is ~0.19 eV, compared to the total available energy [$E_{col}+E_{internal}$(EtOH)+well depth] of 1.50 eV (for En2). Similarly, for the average collision at 0.3 eV, the rotational energy in the precursor is ~0.44 eV, compared to $E_{total}=1.75$ eV. Certainly the rotational energy in the complex is not insignificant, but given the slow increase in L with E_{col}, it seems surprising that angular momentum conservation could completely account for the bottleneck to reaction. We conclude that both vibrational tightness and angular momentum effects probably contribute to suppressing reaction at higher energies.

In this regard, it is somewhat puzzling that there is no rotational effect. There are three possible explanations. One possibility is that angular momentum conservation is, indeed, the major constraint on reaction, and that the rotational angular momentum is simply too small to have a significant effect. The rotational angular momentum is only 10 $\hbar$, compared to the collisional L_{avg} of >100 $\hbar$, and because it adds vectorially, has little effect on the total angular momentum. A second possibility is that the precursor complex potential might be isotropic with respect to NO rotation, such that the nascent rotational energy does not couple in the complex and is not available to drive decomposition. Given the fact that both EtOH and NO^+ have substantial dipole moments, such isotropic interaction is implausible. We tested this idea with a series of *ab initio* single point calculations, in which the NO–EtOH separation was fixed, and the NO was rotated in three orthogonal planes. As expected, the binding is quite anisotropic and we estimate that the barrier to NO^+ rotation within the complex is 0.8–1.25 eV. A third possibility is to invoke some role for dynamics in the precursor complex mechanism discussed previously. As the precursor complex forms, NO^+ rotation will transform into intermolecular bending vibrations. While the additional energy in these vibrations will tend to shorten the complex lifetime, it is possible that bending motion is particularly effective at driving the system through the critical configuration for H^- abstraction (i.e., TS_{HA}).

In summary, the most likely explanation for the sharp collision energy dependence is a tight bottleneck for H^- abstraction. The properties of the complexes in this system suggest a contribution to the bottleneck both from vibrational tightness and angular momentum conservation constraints. Too little is known about the nature of the bottleneck to say with much confidence, why rotation is ineffective. Further quantum chemistry, and perhaps trajectory studies of NO^+–EtOH collisions could presumably resolve this question.

ACKNOWLEDGMENTS

The authors would like to thank Stephen Klippenstein, Alex Boldyrev, William Hase, and Jack Simons for helpful suggestions. This work was supported by the National Science Foundation under Grant No. CHE-9807625. We are also grateful for a grant of computer time from the Utah Center for High Performance Computing. The SGI Origin 2000 used was funded in part by the SGI Supercomputing Visualization.

[1] Y. Ikezoe, S. Matsuoka, M. Takebe, and A. Viggiano, *Gas Phase Ion-Molecule Reaction Rate Constants through 1986* (Mass Spectroscopy Society of Japan, Tokyo, 1987).
[2] W. A. Chupka, M. E. Russell, and K. Refaey, J. Chem. Phys. **48**, 1518 (1968).
[3] C. L. Liao, C. X. Liao, and C. Y. Ng, J. Chem. Phys. **81**, 5672 (1984).
[4] A. Fujii, T. Ebata, and M. Ito, Chem. Phys. Lett. **161**, 93 (1989).
[5] J. Xie and R. N. Zare, J. Chem. Phys. **93**, 3033 (1990).
[6] D. Gerlich and T. Rox, Z. Phys. D: At., Mol. Clusters **13**, 259 (1989).
[7] S. L. Anderson, Adv. Chem. Phys. **82**, 177 (1992).
[8] T. Glenewinkel-Meyer and D. Gerlich, Isr. J. Chem. (in press).
[9] C. W. Eaker and G. C. Schatz, J. Phys. Chem. **89**, 2612 (1985).
[10] L. Zhu and P. Johnson, J. Chem. Phys. **94**, 5769 (1991).
[11] T. P. Softley, S. R. Mackenzie, F. Merkt, and D. Rolland, Adv. Chem. Phys. **101**, 667 (1997).
[12] C. Jouvet, C. Dedonder-Lardeux, S. Martrenchard-Barra, and D. Solgadi, Chem. Phys. Lett. **198**, 419 (1992).
[13] K. F. Willey, C. S. Yeh, and M. A. Duncan, Chem. Phys. Lett. **211**, 156 (1993).
[14] H. Krauss and H. J. Neusser, J. Chem. Phys. **97**, 5923 (1992).
[15] C. W. Hsu, K. T. Lu, M. Evans, Y. J. Chen, C. Y. Ng, and P. Heimann, J. Chem. Phys. **105**, 3950 (1996).
[16] G. Lembach and B. Brutschy, Chem. Phys. Lett. **273**, 421 (1997).
[17] S. R. Mackenzie, E. J. Halse, E. Gordon, D. Rolland, and T. P. Softley, Chem. Phys. **209**, 127 (1996).
[18] S. Sato and K. Kimura, Chem. Phys. Lett. **249**, 155 (1996).
[19] S. R. Mackenzie and T. P. Softley, J. Chem. Phys. **101**, 10609 (1994).
[20] S. R. Mackenzie, E. J. Halse, F. Merkt, and T. P. Softley, Proc. SPIE **2548**, 293 (1995).
[21] J. B. Marquette, C. Rebrion, and B. R. Rowe, J. Chem. Phys. **89**, 2041 (1988).
[22] D. Gerlich, J. Chem. Soc., Faraday Trans. **89**, 2199 (1993).
[23] D. Gerlich and G. Kaffer, Astrophys. J. **347**, 849 (1989).
[24] A. A. Viggiano, R. A. Morris, and J. F. Paulson, J. Chem. Phys. **90**, 6811 (1989).
[25] A. A. Viggiano, J. M. V. Doren, R. A. Morris, J. S. Williamson, P. L. Mundis, and J. F. Paulson, J. Chem. Phys. **95**, 8120 (1991).
[26] C. E. Dateo and D. C. Clary, J. Chem. Soc., Faraday Trans. 2 **85**, 1685 (1989).
[27] I. Dotan, A. A. Viggiano, and R. A. Morris, J. Chem. Phys. **96**, 7445 (1992).
[28] A. A. Viggiano and R. A. Morris, J. Phys. Chem. **100**, 19227 (1996).
[29] K. P. Huber and G. Herzberg, *Molecular Spectra and Molecular Structure. IV. Constants of Diatomic Molecules* (Van Nostrand Reinhold, New York, 1979).
[30] A. D. Williamson and J. L. Beauchamp, J. Am. Chem. Soc. **97**, 5714 (1975).
[31] P. Spanel and D. Smith, J. Chem. Phys. **104**, 1893 (1996).
[32] J. Qian, H. Fu, and S. L. Anderson, J. Phys. Chem. **101**, 6504 (1997).
[33] Y.-h. Chiu, H. Fu, J.-t. Huang, and S. L. Anderson, J. Chem. Phys. **102**, 1199 (1995).
[34] Y.-h. Chiu, H. Fu, J.-t. Huang, and S. L. Anderson, J. Chem. Phys. **102**, 1188 (1995).
[35] H.-T. Kim, R. J. Green, J. Qian, and S. L. Anderson, J. Chem. Phys. **112**, 5717 (2000).
[36] M. J. J. Vrakking and Y. T. Lee, J. Chem. Phys. **102**, 8818 (1995).
[37] F. Merkt and R. N. Zare, J. Chem. Phys. **101**, 3495 (1994).
[38] J. Troe, Chem. Phys. Lett. **122**, 425 (1985).
[39] K. Kimura, S. Katsumata, Y. Achiba, T. Yamazaki, and S. Iwata, *Handbook of HeI Photoelectron Spectra of Fundamental Organic Molecules* (Japan Scientific Societies Press, Tokyo, 1981).
[40] G. Fasano and A. Franceschini, Mon. Not. R. Astron. Soc. **225**, 155 (1987).
[41] S. G. Lias, J. E. Bartmess, J. F. Liebman, J. L. Holmes, and R. D. Levin, J. Phys. Chem. Ref. Data Suppl. **17**, 1 (1988).
[42] M. J. Frisch, G. W. Tucks, H. B. Schlegel, G. E. Scuseria, M. A. Robb, J. R. Cheeseman, V. G. Zakrzewski, J. A. Montgometry, R. E. Stratmann, J. C. Burant, S. Dapprich, J. M. Millam, A. D. Daniels, K. N. Kudin, M. C. Strain, O. Farkas, J. Tomasi, V. Barone, M. Cossi, R. Cammi, B. Mennucci, C. Pomelli, C. Adamo, S. Clifford, J. Ochterski, G. A. Peterson, P. Y. Ayala, Q. Cui, K. Morokuma, D. K. Malick, A. D. Rabuck, K. Raghavachari, J. B. Foresman, J. Cioslowski, J. V. Ortiz, B. B. Stefanov, G. Liu, A. Liashenko, P. Piskorz, I. Komaromi, R. Gomperts, R. L. Martin, D. J. Fox, T. Keith, M. A. Al-Laham, C. Y. Peng, A. Nanayakkara, C. Gonzalez, M. Challacombe, P. M. W. Gill, B. G. Johnson, W. Chen, M. W. Wong, J. L. Andres, M. Head-Gordon, E. S. Replogle, and J. A. Pople, GAUSSIAN 98, Gaussian, Inc., Pittsburgh, PA, 1998.
[43] L. Zhu and W. L. Hase, Quantum Chemical Program Exchange (QCPE), computer program 644.
[44] M. T. Rodgers, K. M. Ervin, and P. B. Armentrout, J. Chem. Phys. **106**, 4499 (1997).
[45] M. T. Rodgers and P. B. Armentrout, J. Chem. Phys. **109**, 1787 (1998).
[46] E. V. Waage and B. S. Rabinovitch, Chem. Rev. **70**, 377 (1970).